biophysica

MDPI

Article

Body Distribution and Occupational Dispersion of Scandium-47 Chloride: Safety Considerations for Radiopharmaceutical Development

Haruna Yorifuji [1], Yoshifumi Shirakami [2], Tadashi Watabe [2], Masashi Murakami [2], Kazuhiro Ooe [3], Kentaro Hisada [1], Atsufumi Akai [1], Sifan Feng [1], Hidetoshi Kikunaga [4], Takuya Yokokita [4], Kazuki Kajiyama [5], Akina Mitsukai [5], Atsushi Toyoshima [5], Takashi Yoshimura [3], Jens Cardinale [6], Frederik L. Giesel [6] and Kazuko Kaneda-Nakashima [1,2,*]

[1] Radiation Biological Chemistry, MS-CORE, Forefront Research Center, Graduate School of Science, The University of Osaka, 2-4 Yakadaoka, Suita 565-0871, Osaka, Japan; akaia26@chem.sci.osaka-u.ac.jp (A.A.)
[2] Institute for Radiation Sciences, The University of Osaka, 1-2 Machikaneyama-cho, Toyonaka 560-0043, Osaka, Japan; yoshifumi_shirakami@irs.osaka-u.ac.jp (Y.S.); watabe.tadashi.med@osaka-u.ac.jp (T.W.); murakami@irs.osaka-u.ac.jp (M.M.)
[3] Radioisotope Research Center, Institute for Radiation Sciences, The University of Osaka, 2-4 Yamadaoka, Suita 565-0871, Osaka, Japan; ooe@rirc.osaka-u.ac.jp (K.O.); tyoshi@rirc.osaka-u.ac.jp (T.Y.)
[4] Research Center for Accelerator and Radioisotope Science (RARiS), Tohoku University, 6-3 Aramaki-Aza, Aoba, Aoba-ku, Sendai 980-8578, Miyagi, Japan; kikunaga@raris.tohoku.ac.jp (H.K.); yokokita@raris.tohoku.ac.jp (T.Y.)
[5] Radiation Sciences, Department of Chemistry, Graduate School of Science, The University of Osaka, 1-1 Machikaneyama-cho, Toyonaka 560-0043, Osaka, Japan; toyo@irs.osaka-u.ac.jp (A.T.)
[6] Nuclear Medicine Department, University Hospital Düsseldorf, Mooren Str. 5, 40225 Düsseldorf, Germany; jens.cardinale@med.uni-duesseldorf.de (J.C.); frederik.giesel@med.uni-duesseldorf.de (F.L.G.)
* Correspondence: kanedak17@chem.sci.osaka-u.ac.jp; Tel.: +81-6-6879-8823

Abstract

This study investigated the distribution and dispersion of Sc-47 (^{47}Sc), a β-emitting radionuclide that can be produced in large quantities using accelerators. As the stability of labeled compounds inside the body is essential for nuclear medicine therapy, we examined the biodistribution of free ^{47}Sc to distinguish it from the distribution of compounds labeled with ^{47}Sc. [^{47}Sc]$ScCl_3$ was administered to normal mice. Body distribution, excretion routes, and contamination of laboratory equipment were also measured. ^{47}Sc remained in the blood for long periods and accumulated mainly in the liver and kidneys because of its binding to plasma proteins. Therefore, ^{47}Sc released from the labeled compounds could potentially cause non-specific liver and kidney damage. Most of the ^{47}Sc was eliminated through feces, whereas some was excreted through the urinary system. ^{47}Sc was found in both the liquid and solid components of the blood. Although animal cages were contaminated with excreta, they could be effectively cleaned by wiping with paper. We also used ^{47}Sc produced by us to label PSMA-617 and verified its performance as a nuclear medicine therapeutic agent. Although [^{47}Sc]Sc-PSMA-617 did not exhibit a high accumulation rate in tumors, it demonstrated antitumor activity. This might suggest the usefulness of ^{47}Sc.

Keywords: scandium-47; distribution; dispersion; nuclear medicine

Check for updates

Academic Editor: Christopher Robinson

Received: 11 June 2026
Revised: 10 July 2026
Accepted: 16 July 2026
Published: 9 August 2026

Copyright: © 2026 by the authors. Licensee MDPI, Basel, Switzerland. This article is an open access article distributed under the terms and conditions of the Creative Commons Attribution (CC BY) license.

1. Introduction

Various radioisotopes are currently used for imaging and therapy in nuclear medicine. Nuclear medicine therapy is a method that can realize "Theranostics," which can perform

"therapy" and "diagnosis" simultaneously. ^{89}Zr [1–3], ^{68}Ga [4], ^{64}Cu [5], and ^{111}In [6] are examples of nuclides for positron emission tomography (PET) [7] or single-photon emission computed tomography (SPECT). ^{177}Lu [8], ^{131}I [9], and ^{90}Y [10] are often used for β-ray nuclide therapy, whereas ^{225}Ac, ^{211}At, and ^{212}Pb are often used for α-ray nuclide therapy [11]. ^{177}Lu is a β-ray nuclide used in nuclear medicine that has attracted considerable attention in recent years. ^{177}Lu ($T_{1/2}$ = 6.65 d) emits β-rays with an average energy of 133.6 keV, making it suitable for use in nuclear medicine. In addition, the main γ-rays of 112.9 and 208.4 keV emitted in conjunction with this are suitable for imaging. However, ^{177}Lu is mainly produced directly by the ^{176}Lu(n,γ)^{177}Lu reaction or indirectly by the ^{176}Yb(n,γ)^{177}Yb $\xrightarrow{\beta^-}$ ^{177}Lu reaction in a nuclear reactor [12,13]. Therefore, in Japan, the supply depends on imports from abroad, which poses challenges in terms of stable supply and transportation costs of the fuel. Therefore, we focused on ^{47}Sc, a β-emitting nuclide that can be produced domestically using an accelerator. The decay schemes and radiations of ^{47}Sc and ^{177}Lu are shown in Figure 1. ^{47}Sc is a nuclide with properties similar to those of ^{177}Lu, including an average β-ray energy (162.0 keV) and half-life (3.35 d) [14]. It also emits 159.4-keV γ-rays that are suitable for imaging. In terms of chemical properties, Sc is a rare earth element similar to Lu and exhibits similar coordination behavior. Therefore, compounds developed for nuclear medicine using ^{177}Lu are considered potentially suitable for ^{47}Sc labeling because of their similar chemical behaviors.

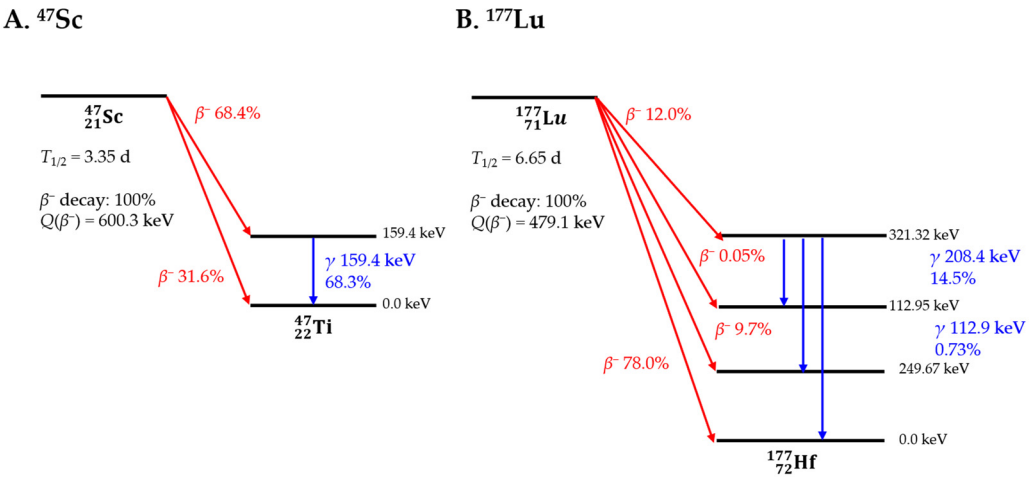


Figure 1. Simplified decay scheme of ^{47}Sc and ^{177}Lu [10].

Scandium has the following characteristics: ^{45}Sc is the only naturally occurring isotope of scandium. Thirteen radioisotopes are known, of which the relatively long-lived radioisotopes are ^{46}Sc ($T_{1/2}$ = 83.8 d), ^{47}Sc ($T_{1/2}$ = 3.35 d), and ^{48}Sc ($T_{1/2}$ = 43.7 h). All remaining half-lives were of less than four hours, and many were of less than two minutes. Collectively, the isotopes of scandium have many excitation states and nuclear isomers, the most stable of which is ^{44m}Sc ($T_{1/2}$ = 58.6 h). The mass numbers of the Sc isotopes ranged from 36 to 71. Those with mass numbers lower than 45 mainly decayed by electron capture, and the decay product was almost entirely Ca. In contrast, those with mass numbers greater than 45 decayed mainly via β-decay, and the decay product was almost entirely Ti. Table 1 lists the radioisotopes of scandium [15–28]. As shown in Table 1, Sc exists in many isomers. Referring to NuDat 3.0, the actual number of reports is up to ^{63}Sc, as listed in Table 1. However, if simulations are included, up to ^{71}Sc has been reported [26]. However, the use of several nuclear isomers remains unknown. Sc is expected to receive considerable attention in the future.

Table 1. Isotopes of Scandium [15–28].

Isotope	Half Life	Decay Mode	Probability	Energy	Refs.
^{36}Sc		p → ^{35}Ca			[15]
^{37}Sc		p → ^{36}Ca			[15]
^{38}Sc	300 ns	p → ^{37}Ca		0.900 MeV	[15]
^{38m}Sc		p → ^{37}Ca			
^{39}Sc	300 ns	p → ^{38}Ca	100%		[15]
^{40}Sc	182.3(7) ms	EC/β^+ → ^{40}Ca EC, p → ^{39}K EC, α → ^{36}Ar	99.54% 0.44% 0.02%	14.320(28) MeV 5.91 MeV 7.279 MeV	[15]
^{41}Sc	596.3(17) ms	EC/β^+ → ^{41}Ca	100%	6.49548(16) MeV	[16]
^{42}Sc	681.79(28) ms	EC/β^+ → ^{42}Ca	100%	6.42609(22) MeV	
^{42m}Sc	61.7(4) s	EC/β^+ → ^{42}Ca	100%		[16]
^{43}Sc	3.891(12) h	EC/β^+ → ^{43}Ca	100%		[16,17]
^{43m1}Sc	438(7) µs	IT → ^{43}Sc			[18]
^{43m2}Sc	472(4) ns				
^{44}Sc	3.93 h	EC/β^+ → ^{44}Ca	100%	3.6527(18) MeV	[16,19]
^{44m1}Sc	154.8(8) ns				[19–21]
^{44m2}Sc	51.0(3) µs				
^{44m3}Sc	58.61(10) h	IT → ^{44}Sc EC/β^+ → ^{44}Ca	98.89(7)% 1.20(7)%	0.271 MeV 3.924 MeV	[22]
^{45}Sc	STABLE				
^{45m}Sc	318(7) ms	IT → ^{45}Sc	100%		[15]
^{46}Sc	83.79(4) d	β^- → ^{46}Ti	100%	2.3666(7) MeV	[19,23]
^{46m1}Sc	9.4(8) µs				[24]
^{46m2}Sc	18.75(4) s	IT → ^{46}Sc	100%		[24]
^{47}Sc	3.3492(6) d	β^- → ^{47}Ti	100%	0.6008(19) MeV	[15,16,19]
^{47m}Sc	272(8) ns				[24]
^{48}Sc	43.67(9) h	β^- → ^{48}Ti	100%	3.989(5) MeV	[19,22]
^{49}Sc	57.2(2) m	β^- → ^{49}Ti	100%	2.0025 MeV	[16,19]
^{50}Sc	1.71 m	β^- → ^{50}Ti	100%	6.884(15) MeV	[25]
^{50m}Sc	0.35(4) s	IT → ^{50}Sc	99.5(5)% <1.0%	6.89 MeV	[19]
^{51}Sc	12.4(1) s	β^- → ^{51}Ti β^-, n → ^{50}Ti	100%	6.504(20) MeV 0.132(20) MeV	[26]
^{52}Sc	8.2 s	β^- → ^{52}Ti	100%	9.03(8) MeV	[26]
^{53}Sc	2.6(4) s	β^- → ^{53}Ti β^-, n → ^{52}Ti	>99.9% <0.1%	7.92(14) MeV 2.49(9) MeV	[26]
^{54}Sc	526(15) ms	β^- → ^{54}Ti β^-, n → ^{53}Ti	86(9) % 16(9) %	11.73(28) MeV 4.87(29) MeV	[26]
^{54m}Sc	2.77(2) µs	IT → ^{54}Sc	100%		[26]
^{55}Sc	92.1 ms	β^- → ^{55}Ti β^-, n → ^{54}Ti	>99.9% <0.1%	11.51(48) MeV 7.39(46) MeV	[26]
^{56}Sc	26(6) ms	β^- → ^{56}Ti β^-, n → ^{55}Ti	100%	14.47(60) MeV 8.74(61) MeV	[26]

Table 1. *Cont.*

Isotope	Half Life	Decay Mode	Probability	Energy	Refs.
^{57}Sc	13(4) ms	$\beta^- \rightarrow {}^{57}$Ti	100%	12.92(133) MeV	[26]
^{58}Sc	12.0 ms	$\beta^- \rightarrow {}^{58}$Ti	100%	16.23(45) MeV	[26]
^{59}Sc	10 ms	$\beta^- \rightarrow {}^{59}$Ti β^-, n $\rightarrow {}^{58}$Ti	100%	12.21(45) MeV 12.74(45) MeV	[26]
^{60}Sc	3 ms	$\beta^- \rightarrow {}^{60}$Ti		17.65 MeV	[26]
^{61}Sc	620 ns	$\beta^- \rightarrow {}^{61}$Ti β^-, n $\rightarrow {}^{60}$Ti β^-, 2n $\rightarrow {}^{59}$Ti		17.28(72) MeV	[26]
^{62}Sc	6.41 ms	$\beta^- \rightarrow {}^{62}$Ti β^-, n $\rightarrow {}^{61}$Ti β^-, 2n $\rightarrow {}^{60}$Ti			[27]
^{63}Sc	4.29 ms	$\beta^- \rightarrow {}^{63}$Ti			[28]

Other radioisotopes of Sc, in addition to ^{47}Sc, which is the focus of this study, are also expected to have applications. Diagnostic and therapeutic radionuclides of the same element (radioisotopes) can be used as chemically identical radiopharmaceuticals for both imaging and subsequent treatment, thereby enabling precise "Theranostics" [17,22]. Sc has three radioisotopes for "Theranostics" applications. ^{43}Sc ($T_{1/2}$ = 3.89 h) and ^{44}Sc ($T_{1/2}$ = 3.97 h) can be used for PET, whereas ^{47}Sc ($T_{1/2}$ = 3.35 d) is suitable for SPECT. Currently, ^{44}Sc is the most advanced isotope in terms of production and preclinical investigations and has been employed in proof-of-concept studies. Although the production of ^{43}Sc may be more challenging, it is advantageous because of the absence of high-energy γ-emissions during its decay.

^{68}Ga is a PET tracer, and ^{225}Ac is produced in small quantities. ^{177}Lu is an excellent isotope for both imaging and therapy; however, owing to the rapidly increasing demand, a stable supply of high-quality material is essential. However, Japan must rely entirely on imports for almost all isotopes. Therefore, we focused on ^{47}Sc that can be produced locally and has similar properties to ^{177}Lu. If the application of the isotope can be shown to be safe, ^{47}Sc may be highly useful [29].

We are developing new nuclear medicine therapeutics, and a stable supply of nuclides is essential for the development of these therapeutics. ^{47}Sc is considered a β-emitting nuclide that can be stably supplied and easily labeled in Japan. We are planning to develop nuclear medicine therapeutics using this nuclide; however, we cannot guarantee the safety of the experimental workers unless we obtain data on the safety and dispersion of the nuclides. Therefore, we measured the distribution and dispersal of this nuclide when administered to experimental animals, as reported previously [30]. Because the sensitivity of radioisotope measurements is very high, it is easy to measure radioisotope-labeled compounds. However, if the radioisotope is free from the compound, it becomes difficult to detect the compound itself because the amount of the compound is too small—unlike with RI. This is because the number of compounds labeled with radioisotopes is typically small. However, if data on nuclides alone are available, it is possible to evaluate the kinetics and stability of the labeled compound by comparing it with nuclide data. If the data are the same, this suggests that the labeling may be incorrect, and further analysis should be performed. This study is expected to provide basic data on the stability of labeled compounds for studying their kinetics in the future. In this study, ^{47}Sc was produced and separated from the target material at Tohoku University and subsequently transported to the University of Osaka. The nuclides were further purified at the Radioisotope Center of the University of Osaka for use in biological experiments. The nuclides were then

resuspended in a liquid state that was safe for use in biological experiments. There is also the study that ^{46}Sc was used instead of ^{47}Sc. This is because ^{47}Sc was difficult to obtain in the past. These studies also suggest high expectations for ^{47}Sc [31].

This study had two objectives. The first was to verify whether our research group could efficiently produce ^{47}Sc, which has recently attracted attention as a nuclide for nuclear medicine therapy, and whether it was possible to manufacture labeled compounds. The second was to obtain distribution data for the radionuclide used for labeling alone to evaluate the in vivo stability of the labeled drugs. Simultaneously, by measuring the actual amount of dispersion and residual levels in the surrounding environment, we aim to acquire data that will help ensure the safety of future research using this radionuclide.

No studies have focused on the issue of dispersion when using nuclear medicine therapy using ^{47}Sc. No previous studies have attempted to quantify the in vivo distribution of ^{47}Sc or the risk of surrounding contamination. Therefore, we believe that our study is valuable because it attempts to examine both the in vivo distribution and risk of dispersion simultaneously.

2. Materials and Methods

2.1. Production and Purification of ^{47}Sc

^{47}Sc was produced via the photonuclear reaction ^{nat}Ti(γ,x)^{47}Sc (where nat indicates natural isotopic abundance) [14] at the Research Center for Accelerator and Radioisotope Science (RARiS), Tohoku University (Sendai, Japan). Natural titanium consists of five stable isotopes (^{46}Ti, ^{47}Ti, ^{48}Ti, ^{49}Ti, and ^{50}Ti). Therefore, irradiation of a ^{nat}Ti target produces several scandium radionuclides in addition to ^{47}Sc. The radionuclidic purity of the product was evaluated by HPGe γ-ray spectrometry before animal administration. The ^{nat}Ti target (5.0 g), packed in a quartz tube, was irradiated with a bremsstrahlung beam with a maximum energy of 30 MeV provided by an electron accelerator at RARiS for 3.5 h. After irradiation, the ^{nat}Ti target was dissolved, and the dissolved solution was processed sequentially using a cation-exchange column followed by a solid-phase extraction column packed with DGA resin (Eichrom Technologies LLC, Lisle, IL USA) to separate ^{47}Sc from the target material. The DGA separation step was repeated twice to maximize the removal of the Ti matrix. Complete removal of Ti was judged qualitatively based on the disappearance of the characteristic color of the Ti-containing solution. After purification, no-carrier-added [^{47}Sc]$ScCl_3$ (hereafter referred to as free ^{47}Sc) was obtained.

2.2. Labeling of PSMA-617 by ^{47}Sc

PSMA-617 was labeled using DOTA as the chelating agent, following the method used for ^{225}Ac labeling. PSMA-617 was purchased from MedChemExpress (Monmouth Junction, South Brunswick, NJ, USA) and dissolved in water (1 mg/mL). All the reagents were purchased from Fujifilm Wako Pure Chemical Corporation. (Tokyo, Japan). In a polypropylene vial, typically, 20 µL of the PSMA-617 aqueous solution, 70 µL of water, 20 µL of 1 mol/L sodium acetate buffer (pH5.0), and 10 µL of [^{47}Sc]$ScCl_3$ solution (5.6 MBq) were added and heated at 80 °C for 1 h. Quality assessment was performed using electrophoresis and high-performance liquid chromatography (HPLC). A small amount of the reaction solution was analyzed by cellulose acetate membrane electrophoresis (electrolyte: 0.06 mol/L barbital buffer, pH8.6, voltage 133 V, current 1 mA/cm, duration: 30 min) and HPLC (SHIMADZU Corp., Kyoto, Japan, column: Cosmosil MSII, 150 × 4.6 mm; eluent: water/MeCN; flow rate: 1 mL/min; detector: UV & RI, gradient: 30% to 60% MeCN, 10 to 30 min).

2.3. Measurements of ^{47}Sc

The radioactivity of the irradiated targets was measured using a high-purity germanium (HPGe) detector (BE2020, Camberra, Mirion Technologies, Inc. ATL, Atlanta, GA, USA) on a single lot. We measured radionuclide purity using a Ge semiconductor detector, and chemical purity was measured using electrophoresis and imaging. Images were captured using a Typhon FLA7000 bioimager (Cytiva, Marlboro, MA, USA). When subsequently administered to the animals, ^{47}Sc was measured using a radioisotope dose calibrator (Curie meter, ICG-8; ALOKA Co., Ltd., Tokyo, Japan). The administered dose was calculated by measuring the dose in a syringe (27G myjector; TERUMO, Inc., Tokyo, Japan) before and after administration. After dissection, the organs were individually placed in polyethylene bags with zippers (A-8, SEISANNIPPONSHA LTD., Tokyo, Japan) and measured using a Wizard^2 2480 γ-counter (PerkinElmer Inc., Waltham, MA, USA). The counting protocol used a 139 to 181 keV (peak 160-keV) energy window and acquired data for 60 s per sample. The distribution of ^{47}Sc in normal mouse organs was evaluated by measuring the radioactivity and correcting for the sample weight. All samples were measured on a semi-microscale (SHIMADZU Corp., Kyoto, Japan).

2.4. Distribution of ^{47}Sc or [^{47}Sc]Sc-PSMA-617 in Mice

ICR mice were used as the normal mice. The mice were supplied by Japan SLC (Hamamatsu, Shizuoka, Japan). Five-week-old male mice were purchased for this study. The animals were maintained on a 12 h light/dark cycle (humidity: 50.0 $\pm$ 5.0%, temperature: 25.0 $\pm$ 0.5 °C). ^{47}Sc was purified as a chloride salt and adjusted with physiological saline to achieve a neutral pH of approximately 7 for administration. After 1 week of habituation, we injected ^{47}Sc via the tail vein (104.47 $\pm$ 3.87 kBq/mouse). The mice were euthanized 10 min, 3 h, 24 h, and 48 h after administration. Twenty mice (31.35 $\pm$ 0.79 g) were used in this study. Each group consisted of five mice. SCID mice implanted with LNCaP cells were used to measure the in vivo distribution of [^{47}Sc]Sc-PSMA-617. SCID mice were purchased from Charles River and acclimated for one week before cell implantation. The detailed procedures followed those described in a published paper. A solution of LNCaP cells at a concentration of 2 $\times$ 10^8 cells/mL was prepared and then mixed with an equal volume of Matrigel. Then, 100 µL of the mixture subcutaneously was injected into the back of each mouse, ensuring a dose of 2 $\times$ 10^7 cells per mouse. Dose measurements were performed in a manner similar to those for ^{47}Sc chloride. The tumor volume at the time of radionuclide administration was 228.2 $\pm$ 69.96 mm^3 in the control group and 247.5 $\pm$ 79.34 mm^3 in the treatment group. We injected [^{47}Sc]Sc-PSMA-617 into the tail vein (1.00 $\pm$ 0.04 MBq/mouse). The mice were euthanized 24 h after administration. Six mice (15.54 $\pm$ 1.63 g) were used in this study. Animal experiments were conducted in accordance with the University of Osaka Animal Experiment Regulations (permission No. 25-007).

2.5. Collection of Feces and Urine from Normal Mice

Basic fecal collection and instrument cleaning were performed as described in previous experiments by Kaneda-Nakashima et al. [30]. However, a more efficient method of collecting feces is to use the equipment shown in Figure 2. Removing feces mixed with bedding is labor-intensive. Polyethylene filter paper (TH-E8401, type A, Chiyoda Technol Corp., Tokyo, Japan) was cut to fit the cage floor, and a wire mesh was placed on top of the floor mesh. The wire mesh prevented the mice from gnawing on the polyethylene filter paper. Using this tool, urine is adsorbed onto the polyethylene filter paper and can be separated without being mixed with feces. All feces were collected using tweezers, placed in a zippered polyethylene bag, and measured with a γ-counter. Urine was calculated as

the sum of what remained in the bladder at the time of autopsy and what was adsorbed onto the polyethylene filter paper.

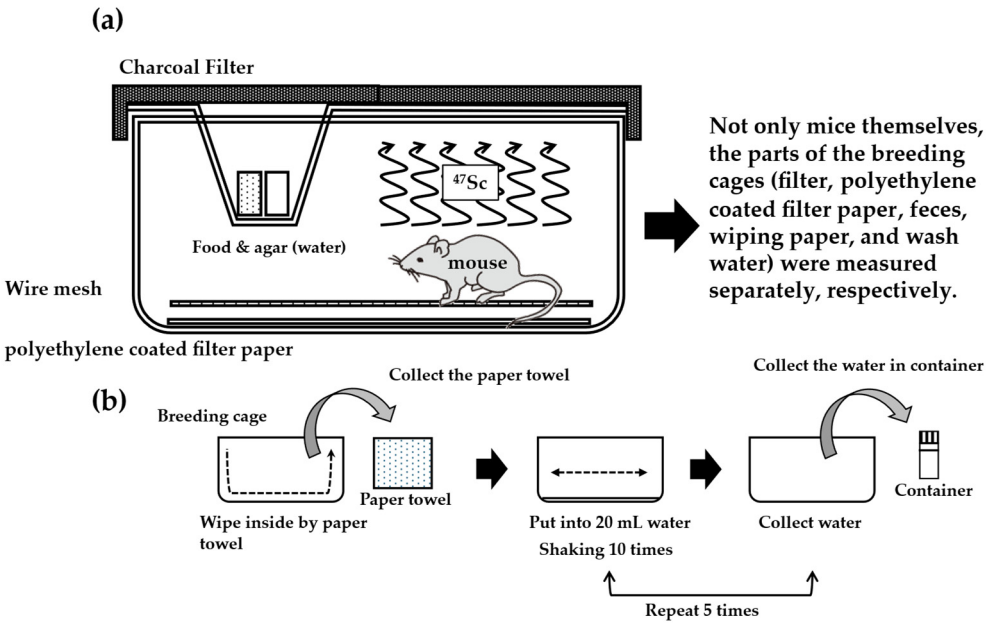


Figure 2. Overview of breeding equipment and cleaning procedures: (**a**) breeding cage and collection of feces and urine. (**b**) Procedure for washing bleeding tools. Samples were collected as previously described. The difference was in the floor bedding. All excreted urine samples were collected and measured using polyethylene filter paper.

After collecting feces and removing the filter paper that had absorbed urine, the cages were wiped with damp paper towels. After wiping the bottom of the cages, the paper towel was folded, and the sides of the cages were wiped. This process was repeated three times, and the paper towels were replaced. The intensity was measured for each wipe. Next, 20 mL of distilled water was added to the cages after wiping was completed, the cages were shaken ten times, and the solution was collected in tubes. This process was repeated five times, and the water was washed five times.

2.6. Electrophoresis

For the analysis of ^{47}Sc in the blood, radioactivity in the plasma was obtained from mice 30 min after intravenous injection. The [^{47}Sc]$ScCl_3$ solution and plasma were analyzed by electrophoresis (strip, cellulose acetate; constant voltage,133 V; constant current, 1 mA/cm; eluent, 0.06 mol/L barbital buffer; pH 8.5; duration, 30 min) as a commonly used and validated method. The radioactivity on the strip was exposed to an imaging plate (Cytiva, Tokyo, Japan), and the migration distance of the radioactivity was measured using a Typhon FLA7000 bioimager.

2.7. Antitumor Effects of [^{47}Sc]Sc-PSMA-617

Model animals were constructed according to standard procedures, and the previously labeled [^{47}Sc]Sc-PSMA-617 was administered intravenously at approximately 3 MBq/mouse (2.84 $\pm$ 0.09 MBq/mouse). Follow-up observations were conducted, and antitumor efficacy was evaluated based on the tumor size.

3. Results

3.1. Quality of Separated ^{47}Sc

Figure 3 shows the γ-ray spectrum of ^{47}Sc measured using a Ge semiconductor detector following the separation and purification processes. In addition to the major γ peak of ^{47}Sc (E_γ = 159.4 keV), relatively weak γ peaks of ^{46}Sc ($T_{1/2}$ = 83.8 d, E_γ = 889.3, 1120.5 keV) and ^{48}Sc ($T_{1/2}$ = 43.7 h, E_γ = 175.4, 983.5, 1037.5, 1312.1 keV) were also observed. These nuclides were produced as by-products of the photonuclear reaction of ^{nat}Ti and could not be chemically separated. The radionuclide compositions of ^{46}Sc, ^{47}Sc, and ^{48}Sc at the end of bombardment were 0.5 ± 0.1%, 87.5 ± 4.7%, and 12.0 ± 1.4%, respectively.

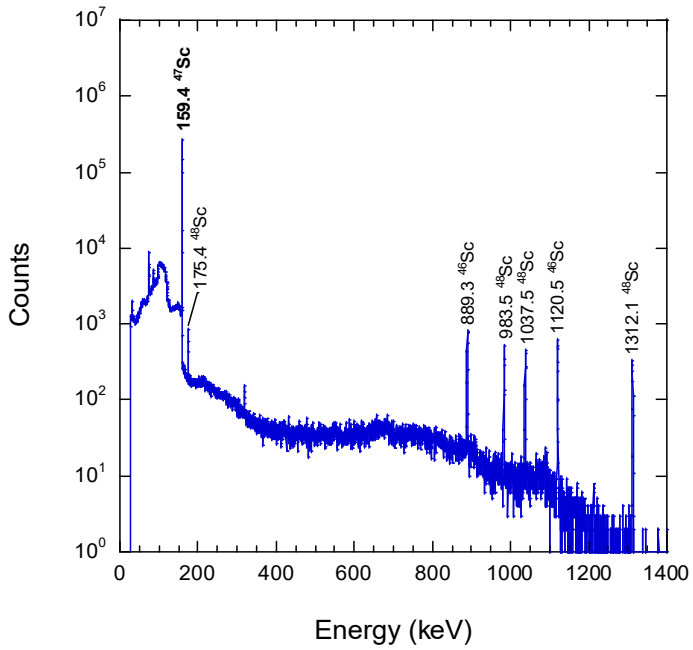


Figure 3. γ-ray spectrum of radioactive scandium chloride solution after purified. The sample was a no-carrier-added [$^{46-48}$Sc]$ScCl_3$ solution sealed in a glass vial with a measured radioactivity of 47.8 ± 1.9 MBq (^{47}Sc) at 265 cm, a measurement time of 180 s (live time), and a dead time of 3.7%.

3.2. Biodistribution of ^{47}Sc in Normal Mice

To minimize the effects of ^{46}Sc and ^{48}Sc, the solution was used eight days after separation. The presence of ^{48}Sc was less than 5% (3.42%) of ^{47}Sc, and the presence of ^{46}Sc decreased to 0.47%, indicating that there would be no significant effects. The biodistribution of ^{47}Sc in normal mice is shown in Table 2 and Figure 4. The accumulation of ^{47}Sc in the brain was low. The accumulation in the thyroid gland increased until 24 h and then decreased. The distribution in the salivary glands, adrenal glands, and thymus was similar to that in the thyroid. ^{47}Sc was first detected in the blood (20.90 ± 2.25%ID/g, 10 min) after intravenous injection, and then gradually decreased (9.08 ± 0.73%ID/g, 3 h). Next, the heart (5.36 ± 0.76%ID/g, 10 min) increased. The dose was then increased in the lungs (8.63 ± 0.76%ID/g, 3 h). The dose transferred to the liver peaked at 24 h and was 31.28 ± 3.74%ID/g. The dose in the gastrointestinal tract was relatively high, resulting in excretion in the feces (14.39 ± 1.78%ID/g, 10 min). The dose in the kidneys (16.65 ± 1.97%ID/g, 24 h) was also high because of the urinary excretion. Based on calculations using the blood intensity, the half-life of [^{47}Sc]$ScCl_3$ was approximately 5.97 h. No organ showed peak accumulation after 48 h [Figure 4]. In addition to measuring distribution, we also measured excretion. The excretion data were shown in Figure 5. Table 3 showed charcoal filter attached to the lid of the breeding cage shown in Figure 2, and Table 4 shows the radiation levels of the cleaning tools.

Table 2. Organ distribution of ^{47}Sc in ICR mice * (%ID/g).

	10 min	3 h	24 h	48 h
Brain	0.49 ± 0.06	0.44 ± 0.18	0.84 ± 0.08	0.32 ± 0.02
Thyroid	1.54 ± 0.24	1.33 ± 0.47	4.10 ± 0.83	1.81 ± 0.23
Salivary gland	1.39 ± 0.25	1.81 ± 0.75	7.55 ± 1.23	3.34 ± 0.42
Heart	5.36 ± 0.76	4.60 ± 1.58	9.18 ± 1.36	3.68 ± 0.28
Lung	6.48 ± 0.80	12.95 ± 6.80	8.63 ± 0.76	2.71 ± 0.30
Thymus	3.53 ± 0.43	2.78 ± 0.93	8.55 ± 1.89	3.53 ± 0.45
Liver	4.12 ± 0.28	16.89 ± 12.10	31.28 ± 3.74	12.88 ± 1.10
Stomach	0.46 ± 0.04	1.98 ± 0.58	5.39 ± 0.55	1.84 ± 0.29
Small intestine	1.38 ± 0.18	3.42 ± 1.21	14.39 ± 1.78	5.81 ± 0.37
Colon	0.72 ± 0.14	1.70 ± 0.67	7.82 ± 1.32	2.06 ± 0.25
Cecum	0.52 ± 0.07	1.38 ± 0.52	5.70 ± 0.78	1.53 ± 0.07
Kidney	5.49 ± 0.39	5.52 ± 1.89	16.69 ± 1.97	6.72 ± 0.45
Adrenal glands	3.03 ± 0.41	3.88 ± 0.73	5.18 ± 1.02	4.49 ± 0.76
Pancreas	1.57 ± 0.20	1.17 ± 0.41	5.14 ± 1.03	1.92 ± 0.30
Spleen	3.80 ± 0.33	8.05 ± 5.60	12.93 ± 1.60	5.30 ± 0.66
Testis	1.12 ± 0.11	2.05 ± 0.74	7.26 ± 0.95	2.98 ± 0.27
Blood	20.90 ± 2.25	13.31 ± 4.47	9.08 ± 0.73	1.11 ± 0.05
Bladder	1.51 ± 0.33	4.20 ± 1.40	4.65 ± 0.99	5.13 ± 1.93
Sternum	2.08 ± 0.09	2.32 ± 0.97	5.02 ± 0.53	2.03 ± 0.19
Spinal cervical	2.42 ± 0.18	2.31 ± 0.76	5.67 ± 0.65	2.43 ± 0.15
Spinal thoracic	2.04 ± 0.15	2.21 ± 0.54	5.57 ± 0.84	2.34 ± 0.23
Rib	3.09 ± 0.19	2.69 ± 0.90	5.96 ± 0.77	2.15 ± 0.10
Femur	1.62 ± 0.18	1.70 ± 0.61	6.49 ± 1.16	3.32 ± 0.30
Skull	1.78 ± 0.21	2.52 ± 0.96	7.60 ± 1.03	3.06 ± 0.30
Upper body residue	1.16 ± 0.11	1.27 ± 0.07	0.90 ± 0.18	0.51 ± 0.07
Lower body residue	1.30 ± 0.04	1.35 ± 0.09	0.53 ± 0.19	0.44 ± 0.02

* All groups consisted of five mice. All data are shown as mean ± S.E. The upper and lower body positions were measured above the pelvis. The femurs were sampled from the left side. The right femur was included in the lower body residue. All values were calculated as %ID/g. ID: injection dose.

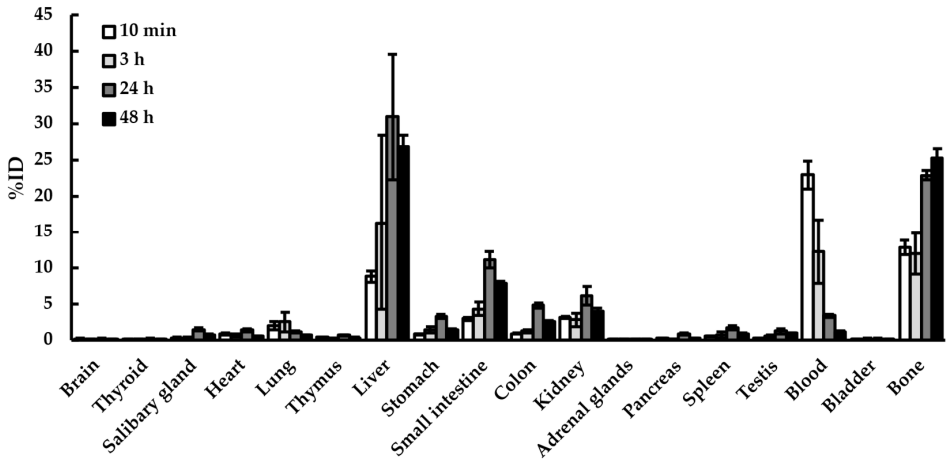


Figure 4. Organ distribution of ^{47}Sc in ICR mice (%ID). Each group consisted of five mice. All data are expressed as the mean ± S.E. The upper and lower body positions were measured above the pelvis. All values were calculated as %ID. ID: injection dose.

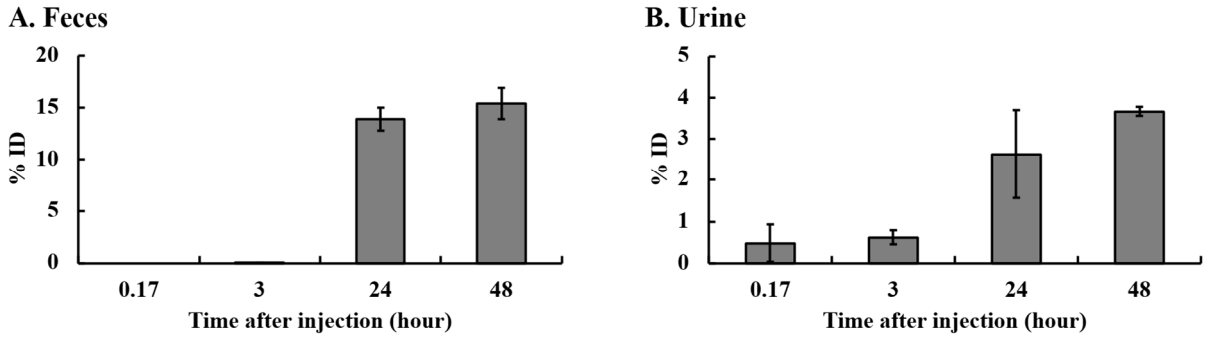


Figure 5. Excretion of ^{47}Sc in ICR mice. The histogram in (**A**) shows the amount excreted in feces, and the graph in (**B**) shows the amount excreted in the urine. The urine volume was calculated as the sum of the value of urine in the bladder and the value of the polyethylene-coated filter paper on which the urine was adsorbed. Data are expressed as the mean ± standard error (S.E.) of five animals. All data are shown as %ID. ID: injection dose.

3.3. Amount of ^{47}Sc in Blood

The amount of ^{47}Sc in the blood after 10 min was high. After blood collection, heparin was added, and the mixture was centrifuged to separate the serum and blood cells. The respective doses were measured. The results showed that exactly half (50.99 ± 2.07%) of the active radiation was detected in the liquid component, suggesting that some ^{47}Sc was taken up by blood cells, such as white blood cells, platelets, and red blood cells, whereas the remainder existed in the liquid component. The stability data using blood components by electrophoresis are shown in Figure 6.

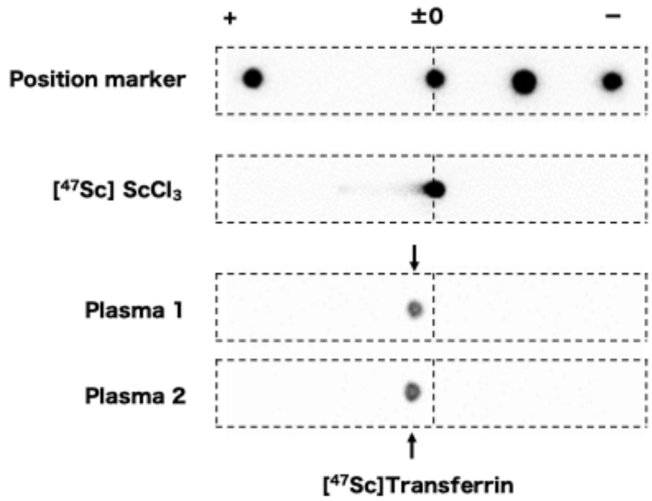


Figure 6. Electrophoresis of ^{47}Sc. [^{47}Sc]$ScCl_3$ and plasma were mixed with ^{47}Sc. Plasma was collected from normal mice. The left and right sides represent the anodes and cathodes, respectively. The top row shows the electrophoresis results of the location marker, ^{47}Sc scandium chloride, mixed with plasma 1, and the sample mixed with plasma 2.

3.4. Efficacy of [^{47}Sc]Sc-PSMA-617

Table 5 [32–38] shows that compounds that prostate specific membrane antigen (PSMA), a known marker for prostate cancer cells, are also attracting attention as targets for the development of nuclear medicine therapeutics using ^{47}Sc. We therefore conducted our study using PSMA-617. The structure of [^{47}Sc]Sc-PSMA-617 is shown in Figure 7. When the reaction mixture of PSMA-617 was subjected to electrophoresis, [^{47}Sc]Sc-PSMA-617 was detected at a migration distance of +30 mm with a high radiochemical yield (RCY: 96.7%) [Figure 7]. Meanwhile, [^{47}Sc]Sc-PSMA-617 was eluted at 19.4 min by HPLC analysis

[Figure 7]. To achieve not less than 90% RCY, 20 mmol of ligand was required for labeling at pH 5.0, whereas 300 mmol of ligand was required at pH 6.5.

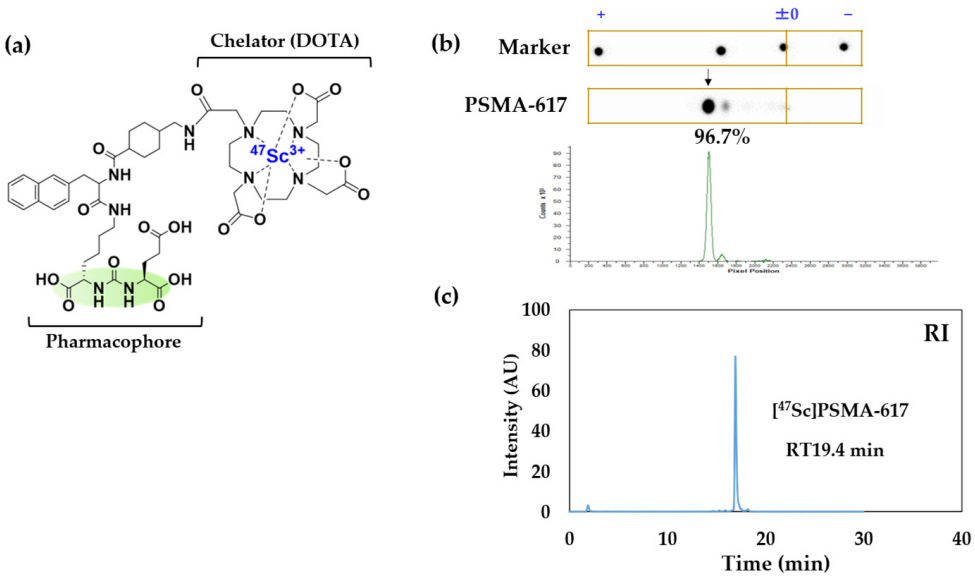


Figure 7. Structure and quality of [^{47}Sc]Sc-PSMA-617. (**a**) The structure of [^{47}Sc]Sc-PSMA-617. The chelator is DOTA, and the pharmacophore is shown in green. (**b**) Electrophoresis results of [^{47}Sc]Sc-PSMA-617. (**c**) HPLC analysis results of [^{47}Sc]Sc-PSMA-617. Radiochemical Purity (RCP) of [^{47}Sc]Sc-PSMA-617 was 96.7%.

Table 6 shows the organ distribution of [^{47}Sc]Sc-PSMA-617 in the tumor model 24 h post-administration. This represents the cumulative amount over 24 h. Approximately 40% was excreted in the urine (40.83 ± 3.03%ID).

Table 3. ^{47}Sc in a charcoal filter attached to the lid of the breeding cage.

	%ID
0 min–10 min	$1.3 \times 10^{-2} \pm 3.9 \times 10^{-3}$
10 min–3 h	$3.4 \times 10^{-3} \pm 3.2 \times 10^{-4}$
3h–24 h	$1.7 \times 10^{-2} \pm 3.9 \times 10^{-3}$
24 h–48 h	$1.7 \times 10^{-2} \pm 2.6 \times 10^{-5}$

%ID; % of injection dose. The table indicates the amount excreted during expiration per animal. Indicates the dose adsorbed on activated charcoal divided by the dose administered (N = 5).

Table 4. ^{47}Sc intensity of cleaning tools (%ID).

Times	10 min	3 h	24 h	48 h
Towel 1st	$3.9 \times 10^{-2} \pm 1.2 \times 10^{-4}$	$4.2 \times 10^{-2} \pm 1.4 \times 10^{-4}$	$6.6 \times 10^{-2} \pm 1.1 \times 10^{-5}$	$3.9 \times 10^{-2} \pm 2.3 \times 10^{-5}$
Towel 2nd	$1.3 \times 10^{-2} \pm 1.1 \times 10^{-4}$	$8.6 \times 10^{-3} \pm 1.1 \times 10^{-5}$	$2.8 \times 10^{-2} \pm 1.0 \times 10^{-5}$	$1.2 \times 10^{-2} \pm 4.2 \times 10^{-5}$
Towel 3rd	$4.4 \times 10^{-3} \pm 1.3 \times 10^{-5}$	$5.7 \times 10^{-3} \pm 1.0 \times 10^{-5}$	$1.8 \times 10^{-2} \pm 2.1 \times 10^{-6}$	$3.9 \times 10^{-3} \pm 1.7 \times 10^{-5}$
Water 1st	$2.6 \times 10^{-3} \pm 1.1 \times 10^{-5}$	$1.3 \times 10^{-3} \pm 1.2 \times 10^{-6}$	$3.4 \times 10^{-3} \pm 1.2 \times 10^{-6}$	N.D.
Water 2nd	$6.4 \times 10^{-4} \pm 1.2 \times 10^{-6}$	$7.5 \times 10^{-4} \pm 1.1 \times 10^{-6}$	$1.5 \times 10^{-3} \pm 1.1 \times 10^{-6}$	$1.5 \times 10^{-3} \pm 1.4 \times 10^{-6}$
Water 3rd	$4.0 \times 10^{-4} \pm 2.3 \times 10^{-6}$	$5.2 \times 10^{-4} \pm 1.3 \times 10^{-6}$	N.D.	N.D.
Water 4th	$4.4 \times 10^{-4} \pm 2.3 \times 10^{-6}$	N.D.	$8.6 \times 10^{-4} \pm 1.3 \times 10^{-6}$	$1.3 \times 10^{-3} \pm 3.1 \times 10^{-6}$
Water 5th	$1.6 \times 10^{-4} \pm 2.0 \times 10^{-6}$	N.D.	$9.7 \times 10^{-4} \pm 1.0 \times 10^{-6}$	$4.5 \times 10^{-4} \pm 1.1 \times 10^{-7}$

%ID; % of injection dose. N.D.; not detected. Paper towels for wiping were moistened and used one at a time, and 20 mL of wash water was used each time.

Table 5. Reports of ^{47}Sc labeling experiment.

Author	Material	Target	Source
Kim et al. [32]	Cetuximab	Lung cancer (EGFR)	BMC Cancer. 2023; 23(1): 652.
Nardo et al. [33]	Folate (cm10)	Various cancer (Folate receptor)	Phys Med Biol. 2021; 66(2): 025003.
Vaughn et al. [34]	picaga-Alb53-PSMA PSMA-617	Prostate cancer (PSMA)	Mol Pharm. 2021; 18(12): 4511–4519.
Meier et al. [35]	PSMA-617	Prostate cancer (PSMA)	Molecules. 2023; 28(16): 6041.
Garnuszek P et al. [36]	PSMA-D4	Prostate cancer (PSMA)	Int J Mol Sci. 2021; 22(5): 2731.
Moghaddam-Banaem et al. [37]	Risedronate	Osteoporosis	Radiat Prot Dosimetry. 2022; 198(19): 1483–1494.
Cingoranelli et al. [38]	PSMA-617	Prostate cancer (PSMA)	Mol Pharm. 2026; 23(3): 1517–1528

Table 6. Organ distribution of ^{47}Sc in SCID (LNCaP model) mice * (%ID/g).

	24 h
Brain	0.03 ± 0.0027
Thyroid	0.08 ± 0.0015
Salivary gland	0.19 ± 0.012
Heart	0.19 ± 0.023
Lung	1.48 ± 0.17
Tumor	1.16 ± 0.13
Liver	1.89 ± 0.15
Stomach	0.35 ± 0.041
Small intestine	1.57 ± 0.37
Colon	2.99 ± 0.76
Kidney	1.07 ± 0.23
Pancreas	0.11 ± 0.0083
Spleen	1.16 ± 0.10
Testis	0.16 ± 0.016
Blood	0.21 ± 0.039
Bone	0.22 ± 0.039
Upper body residue	0.16 ± 0.0066
Lower body residue	0.20 ± 0.013

* All groups consisted of %ID/g. All data are expressed as the mean ± S.E. Upper and lower body positions were measured above the pelvis. All values were calculated as %ID/g. ID: injection dose.

3.5. Absorbed Doses to Organs

The absorbed doses to organs were calculated using the IDAC-Dose 2.1 software [Table 7] (https://www.idac-dose.org/) [39]. The access date was 1 May 2026.

Table 7. Absorbed doses per unit activity administered for $^{47}ScCl_3$ (mGy/MBq).

Organs	Absorbed Dose of [^{47}Sc]$ScCl_3$ (mGy/MBq)	
	Male	Female
Adrenals	0.206	0.270
Brain	0.026	0.029
Breast	0.038	0.035

Table 7. *Cont.*

Organs	Absorbed Dose of [^{47}Sc]$ScCl_3$ (mGy/MBq)	
	Male	**Female**
Colon wall	0.085	0.071
Endosteum (bone surface)	0.028	0.040
Gallbladder wall	0.322	0.375
Heart wall	0.117	0.149
Kidneys	1.460	1.730
Liver	1.820	2.340
Lung	0.223	0.271
Muscle	0.016	0.029
Pancreas	0.465	0.535
Red (active) bone marrow	0.067	0.095
Salivary glands	0.965	1.180
Skin	0.016	0.021
Small intestine wall	0.077	0.095
Spleen	0.600	0.739
Stomach wall	0.126	0.166
Effective dose 60 [mGy/MBq]	0.194	0.246

4. Discussion

In this study, ^{47}Sc was produced via the photonuclear reaction on natural titanium using bremsstrahlung from an electron linear accelerator. Several studies have reported the production of 4^{7}Sc using similar photonuclear reactions at various endpoint energies [40–42]. Hovhannisyan et al. (2022) conducted irradiations using bremsstrahlung with an endpoint energy of 30 MeV, which is the same energy employed in this study [42]. They reported that, at the end of a one-hour irradiation, the radionuclidic impurities 46Sc and 48Sc accounted for 1.3% and 9.1% of the ^{47}Sc activity, respectively. In our study, as described in Section 2.1, the cor-responding values were 0.6 ± 0.1% for ^{46}Sc and 13.7 ± 1.8% for ^{48}Sc, showing a broadly comparable radionuclidic composition. As noted by Hovhannisyan et al., the use of en-riched ^{48}Ti targets instead of natural titanium would likely improve the radionuclidic purity [43].

[^{44}Sc]$ScCl_3$ has been reported to be used in Swiss Webster mice [44]. The background of these mice was almost the same as that of the ICR mice used in this study. Compared with the [^{44}Sc]$ScCl_3$ data, in blood, heart, lung, liver, kidneys and spleen, the accumulation peak of [^{47}Sc]$ScCl_3$ was 24 h. However, since [^{44}Sc]$ScCl_3$ and [^{47}Sc]$ScCl_3$ are chemically identical, there should be no difference in their distribution in the body. For example, it is known that protein binding rates differ among species and strains [45]. Furthermore, chemical impurities, if any, may also have an effect, but since $ScCl_3$ is a simple compound, the effect is unlikely to be significant. Analysis of the excretion profile showed biological half-life of [^{47}Sc]$ScCl_3$ might be shorter than its physical half-life. Free [^{47}Sc]$ScCl_3$ was also excreted primarily through the liver (24 h; 31.28 ± 3.74%ID/g), and portion through the kidneys (24 h; 16.69 ± 1.97%ID/g). Because of the relatively high accumulation in the liver, even after 48 h, there is concern that side effects may occur due to the approximately 3 d half-life of this radionuclide. When the liver is exposed to high doses of radiation, direct damage to liver blood vessels and cells, impaired blood flow in the liver, and necrosis of hepatocytes may occur due to radiation. The presence or absence of non-specific accumulation in the liver must be confirmed when considering the localization of a labeled substance as a therapeutic agent. Low background levels of ac-cumulation were measured in all other collected organs, including thyroid, bone, brain, salivary glands, and stomach. The major difference is that, unlike the distribution of [^{44}Sc]ScCl3, our results also showed

accumulation in the gastrointestinal tract. The accumulation in the stomach, small intestine, and large intestine was highest at 24 h [Table 2]. The Main reason for the higher doses in the digestive tract in our data was that we measured the contents of the digestive tract as they were. The most likely route of transfer of the dose to the gastrointestinal tract contents might be that after entering the bloodstream, the dose was metabolized in the liver and excreted into the bile. The bile was then stored in the gallbladder and discharged into the duodenum, resulting in the excretion of unabsorbed drugs and metabolites as feces. Scandium administered intravenously binds to apo-transferrin, is carried by the bloodstream to the liver, and accumulates there temporarily. Since the liver is the site for the synthesis of metalloproteins and metalloenzymes, scandium is distributed to the liver, and a portion is thought to be excreted in urine or feces [Figure 5]. Although scandium is a rare earth element, it showed excretion behavior similar to that of transition metals [46]. Although the reason for the migration of the labeled compound into the intestinal tract during intravenous administration requires further study, the experimental results obtained in this study are important for evaluating the stability of ^{47}Sc-labeled compounds in the body. On the other hand, it is assumed that ^{47}Sc is excreted in the urine as $^{47}Sc^{3+}$ ions (free ^{47}Sc); however, this has not yet been confirmed by TLC or other analyses. To clarify the properties of ^{47}Sc in vivo, further analysis is required.

Regarding the experimental materials and their dispersal into the surrounding environment, it was confirmed that there was no significant risk when using the appropriate materials and existing containment procedures. However, handling high-dose materials requires caution. Examples include blood and urine. Blood accumulation was considerably high, even after 10 min [Table 2]. Subsequently, these values decreased gradually. This is a good indication that scandium is in the bloodstream and that it passes through the circulatory system. ^{47}Sc is then excreted through the excretory organs, kidneys, feces, and urine. As the peak accumulation in all organs except the blood was at 24 h, excretion up to 24 h should be noted for contamination during the experiment. The high excretion in the blood and urine indicates that one must be more careful owing to contamination [Figure 5]. ^{47}Sc was barely detectable in exhaled breath, and Table 3 shows that the amount of adsorption remained almost the same from 10 min to 48 h. We confirmed that the low values in activated carbon filters attached to the cage lids when rearing isotopically administered animals [Table 3]. Furthermore, the amount of ^{47}Sc detected was just below the detection limit for five animals, and even when converted per animal, the amount was lower than 0.05%ID. In other words, the dispersal of exhaled breath or urine evaporated from the bedding of the administered animals was minimal. Metabolic cages were used to collect urine and feces. Feces must also be treated as a source of contamination. The usefulness of wiping was also confirmed. Simply wiping the cage reduced contamination by approximately 1/10 [Table 4]. Vessel surface contamination can be reduced by wiping. Water contamination can be reduced by wiping. All radioactive waste generated during this study was managed in accordance with institutional radiation safety regulations.

Table 5 lists the studies conducted to date on the application of ^{47}Sc in nuclear medicine [32–38]. Most of these agents are related to the prostate-specific membrane antigen (PSMA), which is the molecular target of prostate cancer. This may be because the precursor used for labeling ^{225}Ac or ^{177}Lu was DOTA. The same precursor used for labeling with ^{225}Ac or ^{177}Lu can be used to label ^{47}Sc. Because only a few new reports are available, further studies on this nuclide are required. We must consider the implications of the difference between ^{47}Sc and the ligand, that is, the compound labeled with ^{47}Sc. In other words, the biodistribution of ^{47}Sc alone shows the distribution of Sc off the ligand, that is, when the labeled compound is unstable. A labeled compound with a distribution similar to that of ^{47}Sc alone cannot be guaranteed to be stable as a labeled compound. A

previous study compared ^{177}Lu and ^{47}Sc using PSMA as the molecular target [34]. In that study, a highly selective PSMA compound was labeled with ^{47}Sc to confirm its in vivo behavior. Moreover, the retention of the compound in the liver and blood was significantly lower. This suggests that the behavior varies significantly depending on the compound to be labeled. When evaluating labeled compounds, attention should be paid to blood and liver damage and the purity of the labeled compound. This is because if the labeling of the compound is unstable, ^{47}Sc removed from the compound is expected to accumulate in the blood and liver, as shown in Table 2. The distribution of ^{47}Sc is quite different from that of the α-ray-emitting nuclides (^{211}At, ^{223}Ra, and ^{225}Ac) studied in our previous study [30]. The retention of these metals in the blood was very high [Table 2]. Scandium chloride is water-soluble. Once administered into the body, ^{47}Sc might immediately bind to apo-transferrin [47,48]. This ^{47}Sc-transferrin is distributed via transferrin receptors expressed on cells to large organs of the blood pool, liver, kidneys, etc. (taken up into cells by endocytosis.) The distribution of ^{47}Sc is probably in cells (i.e., iron-rich) and organs with high transferrin expression (i.e., iron-rich cells like red blood cells). Figure 6 shows the electrophoresis results of the plasma after treatment. This indicates that the ^{47}Sc spots moved to the β-fraction. This result suggests that ^{47}Sc binds to transferrin, similar to existing reports [44], and consequently, its retention in the blood increases. The higher excretion in feces than in urine is attributed to biliary excretion. It is thought to diffuse into the body through blood circulation and then be metabolized in the liver. ^{47}Sc is also expected to be a therapeutic agent for osteoporosis relief. When a compound accumulated in the bone (1,4,7,10-tetraazacyclododecane-1,4,7,10-tetramethylene phosphonic acid) [31], ^{47}Sc also showed strong accumulation in the bone [Table 2], indicating its potential for future use in bone imaging.

Compared with ^{47}Sc, [^{47}Sc]Sc-PSMA-617 exhibited markedly different accumulation [Tables 2 and 6; Figures 7 and 8]. The urinary excretion of [^{47}Sc]Sc-PSMA-617 over 24 h averaged 40.83 ± 1.75%ID. This is markedly different from the 2.63 ± 1.07%ID of ^{47}Sc excreted over 24 h in normal mice [Figure 5]. The ^{47}Sc was distributed in normal organs, particularly the liver and bone (sum of multiple sites) [Figure 4]. However, after 24 h, almost none of the [^{47}Sc]Sc-PSMA-617 remained in the body [Figure 8]. The stability of the labeled compound is critical for ensuring the safety of radiopharmaceuticals. The bone-to-blood ratio was 1.04 for ^{47}Sc, compared to 3.09 for [^{47}Sc]Sc-PSMA-617, indicating reduced accumulation in the bone. The fact that the amount of urinary excretion was so high and rapid excretion is desirable for a pharmaceutical product, it was confirmed that consideration must be given to the safety of healthcare professionals working with patients. The pharmacokinetics of [^{47}Sc]Sc-PSMA-617 were similar to those of ^{68}Ga-PSMA-617, and it was rapidly excreted from the body [49]. The non-specific organ accumulation of [^{47}Sc]Sc-PSMA-617 was low. Although tumor accumulation was not as high as anticipated in this study, a certain degree of therapeutic effect was observed [Figure 9], suggesting that the clearance of [^{47}Sc]Sc-PSMA-617 was likely very rapid. A comparison with ^{47}Sc distribution data demonstrated the instability of our labeled compound. Without ^{47}Sc data, it would be difficult to determine the stability of ^{47}Sc-labeled compounds in vivo. Data on the labeled nuclide alone were useful for evaluating the stability of the labeled compound and its potential side effects. A comparison of Figures 2 and 4 shows that ^{47}Sc chloride tends to accumulate in the bone and liver, whereas [^{47}Sc]Sc-PSMA-617 was rapidly cleared. Accumulation in the liver may serve as an indicator for evaluating the stability of ^{47}Sc-labeled compounds. Table 2 shows that there was a high accumulation in bone tissue, with few differences depending on the site of measurement.

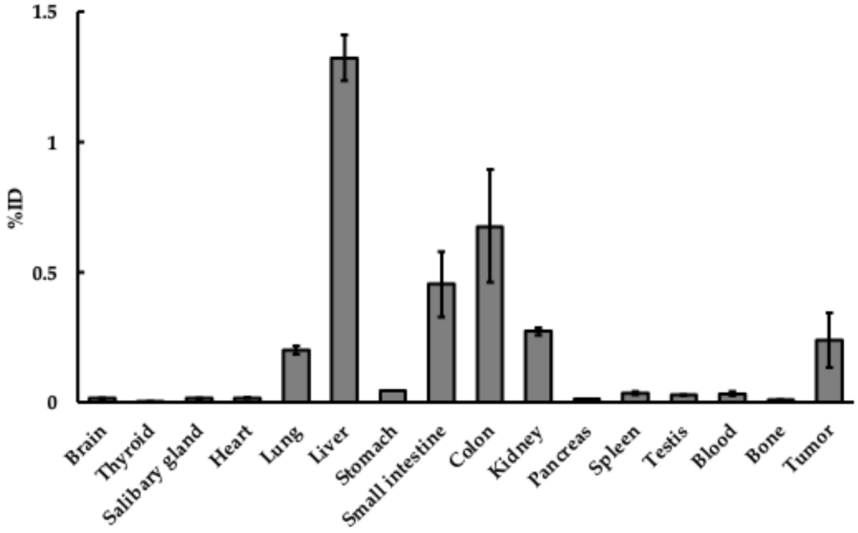


Figure 8. Organ distribution of [^{47}Sc]Sc-PSMA-617 in SCID mice (%ID). Each group consisted of three mice. All data are expressed as the mean ± S.E. The upper and lower body positions were measured above the pelvis. All values were calculated as %ID. ID: injection dose.

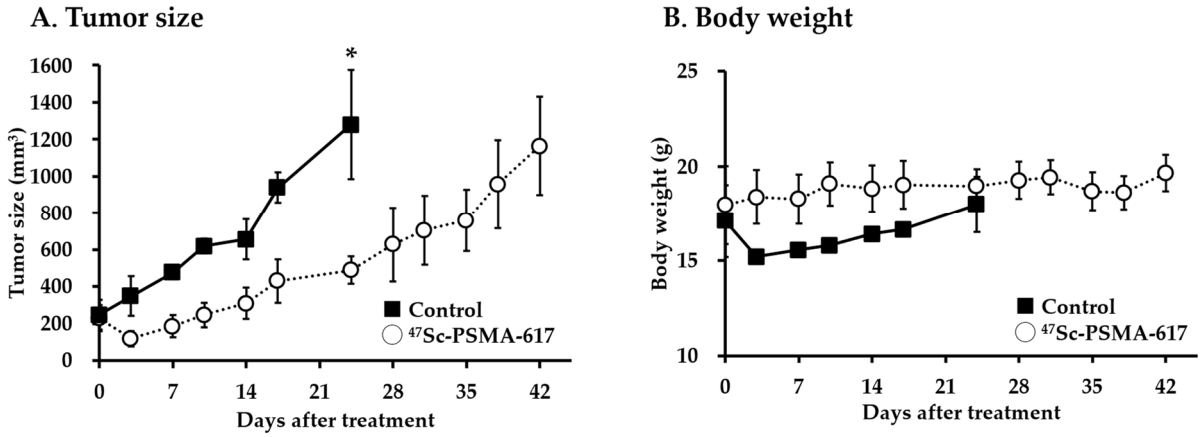


Figure 9. Evaluation of the anticancer effect of [^{47}Sc]Sc-PSMA-617. The solid lines with black squares represent the control group, and the dotted lines with white circles represent the group treated with [^{47}Sc]Sc-PSMA-617. (**A**) shows tumor size, and (**B**) shows body weight. For the control group, the threshold was set at the point where the tumor exceeded 10% of body weight, and the same threshold was applied to the treatment group. * $p < 0.05$.

It is true that there are specific radionuclides suited for imaging or treatment. The benefits of ^{47}Sc in nuclear medicine therapy are that it does not require the use of other nuclides for imaging, as ^{47}Sc can be imaged using the 159 keV γ-rays it emits, and dosimetry is possible. In other words, the advantage of ^{47}Sc is that both imaging and therapy can be performed using the same isotopes.

5. Conclusions

Japan, since domestic mass manufacturing methods of ^{177}Lu are under consideration [50,51], relies on imports for the supply of that nuclide. Thus, we turned our attention to ^{47}Sc, which can be produced domestically. This is because, like ^{177}Lu, ^{47}Sc can be labeled in compounds and used for imaging. The absorbed dose of ^{47}Sc was higher than that of ^{44}Sc in the kidneys, liver, and spleen [44]. In other words, if the radiolabeled compound is unstable, adverse effects are likely to be more pronounced in these organs. In our study, when we extrapolated the absorbed dose to humans, the absorbed dose of ^{47}Sc was higher in the kidneys and liver [Table 7]. The high blood retention of ^{47}Sc [52] and significant

accumulation in the liver and kidneys are of major concern for radiopharmaceutical stability assessment. Because of that, before evaluating labeled compounds using a new radionuclide, it is essential to first examine the distribution of the radionuclide on its own.

Author Contributions: Conceptualization, K.K.-N. and Y.S.; methodology, M.M. and K.K.-N.; software, M.M.; validation, M.M., K.K. and A.M.; formal analysis, M.M.; investigation, H.Y., K.H., A.A., S.F., Y.S. and K.K.-N.; resources, M.M., H.K., T.Y. (Takuya Yokokita), K.K., A.M., A.T., J.C. and F.L.G.; data curation, K.K.-N. and K.H.; writing—original draft preparation, H.Y. and K.K.-N.; writing—review and editing, H.Y., K.H., S.F. and K.K.-N.; visualization, M.M. and K.K.-N.; supervision, K.O. and T.Y. (Takashi Yoshimura); project administration, T.W., M.M. and K.K.-N.; funding acquisition, A.T. and T.W. All authors have read and agreed to the published version of the manuscript.

Funding: This work was supported by the Research Program in Research Center for Accelerator and Radioisotope Science, Tohoku University (proposal No. 3071). This study was also funded by the commissioned research fund provided by F-REI (JPFR25040302).

Institutional Review Board Statement: The animal study protocol was approved by the Institutional Review Board of the Institute for Radiation Sciences at the University of Osaka (protocol No. 25-007 and date of approval: 1 April 2025) for studies involving animals.

Informed Consent Statement: Not applicable.

Data Availability Statement: No new data were created or analyzed in this study. Data sharing is not applicable to this article.

Acknowledgments: We thank H. Egawa, T. Kobayashi and A. Saito-Kawakami for their great cooperation in conducting this experiment.

Conflicts of Interest: The authors declare no conflicts of interest.

References

1. Deri, M.A.; Zeglis, B.M.; Francesconi, L.C.; Lewis, J.S. PET imaging with ^{89}Zr: From radiochemistry to the clinic. *Nucl. Med. Biol.* **2013**, *40*, 3–14. [CrossRef] [PubMed]
2. Yoon, J.K.; Park, B.N.; Ryu, E.K.; An, Y.S.; Lee, S.J. Current Perspectives on $^{(89)}$Zr-PET Imaging. *Int. J. Mol. Sci.* **2020**, *21*, 4309. [CrossRef] [PubMed]
3. Wuensche, T.E.; Lyashchenko, S.; van Dongen, G.A.M.S.; Vugts, D. Good practices for ^{89}Zr radiopharmaceutical production and quality control. *EJNMMI Radiopharm. Chem.* **2024**, *9*, 40. [CrossRef] [PubMed]
4. Wu, G.; Wang, D.; Zhang, W.; Jia, Z.; Li, J.; Zhang, L. Head-to-head comparison of [^{68}Ga]Ga-FAPI PET and [^{18}F]FDG PET in the detection of bone and lymph node metastasis in various cancers: A systematic review and meta-analysis. *Eur. J. Radiol.* **2024**, *171*, 111302. [CrossRef] [PubMed]
5. Yang, N.; Guo, X.Y.; Ding, J.; Wang, F.; Liu, T.L.; Zhu, H.; Yang, Z. Copper-64 Based PET-Radiopharmaceuticals: Ways to Clinical Translational. *Semin. Nucl. Med.* **2024**, *54*, 792–800. [CrossRef] [PubMed]
6. Crișan, G.; Moldovean-Cioroianu, N.S.; Timaru, D.G.; Andrieș, G.; Căinap, C.; Chiș, V. Radiopharmaceuticals for PET and SPECT Imaging: A Literature Review over the Last Decade. *Int. J. Mol. Sci.* **2022**, *23*, 5023. [CrossRef] [PubMed]
7. Kim, S.Y.; Chung, H.W.; So, Y.; Lee, M.H.; Lee, E.J. Recent Updates of PET in Lymphoma: FDG and Beyond. *Biomedicines* **2024**, *12*, 2485. [CrossRef] [PubMed]
8. Ahmadzadehfar, H.; Seifert, R.; Afshar-Oromieh, A.; Kratochwil, C.; Rahbar, K. Prostate Cancer Theranostics With $^{(177)}$Lu-PSMA. *Semin. Nucl. Med.* **2024**, *54*, 581–590. [CrossRef] [PubMed]
9. Manzil, F.F.P.; Kaur, H. Radioactive Iodine Therapy for Thyroid Malignancies. In *StatPearls [Internet]*; StatPearls Publishing: Treasure Island, FL, USA, 2024.
10. Yu, C.Y.; Huang, P.H.; Tsang, L.L.C.; Hsu, H.W.; Lim, W.X.; Weng, C.C.; Huang, T.L.; Hsu, C.C.; Chen, C.L.; Ou, H.Y.; et al. Yttrium-90 Radioembolization as the Major Treatment of Hepatocellular Carcinoma. *J. Hepatocell. Carcinoma* **2023**, *10*, 17–26. [CrossRef] [PubMed]
11. Song, H.; Sgouros, G. Alpha and Beta Radiation for Theragnostics. *PET Clin.* **2024**, *19*, 307–323. [CrossRef] [PubMed]
12. Rahman, A.K.M.R.; Amin, R. Production route analysis of a therapeutic radionuclide ^{177}Lu. *AIP Adv.* **2022**, *12*, 095115. [CrossRef]
13. Dash, A.; Pillai, M.R.A.; Knapp, F.F., Jr. Production of ^{177}Lu for Targeted Radionuclide Therapy: Available Options. *Nucl. Med. Mol. Imaging* **2015**, *49*, 85–107. [CrossRef] [PubMed]

14. Burrows, T.W. Nuclear data sheets for A=47. *Nucl. Data Sheets* **2007**, *108*, 923–1056. [CrossRef]
15. NuDat 3.0, National Nuclear Data Center, Brookhaven National Laboratory. Available online: https://www.nndc.bnl.gov/nudat3/ (accessed on 8 July 2025).
16. Szkliniarz, K.; Sitarz, M.; Walczak, R.; Jastrzębski, J.; Bilewicz, A.; Choiński, J.; Jakubowski, A.; Majkowska, A.; Stolarz, A.; Trzcińska, A.; et al. Production of medical Sc radioisotopes with an alpha particle beam. *Appl. Radiat. Isot.* **2016**, *118*, 182–189. [CrossRef] [PubMed]
17. Müller, C.; Domnanich, K.A.; Umbricht, C.A.; van der Meulen, N.P. Scandium and terbium radionuclides for radiotheranostics: Current state of development towards clinical application. *Br. J. Radiol.* **2018**, *91*, 20180074. [CrossRef] [PubMed]
18. Schmidt-Ott, W.D.; Asahi, K.; Fujita, Y.; Geissel, H.; Gross, K.D.; Hild, T.; Irnich, H.; Ishihara, M.; Krumbholz, K.; Kunze, V.; et al. Spin alignment of ^{43}Sc produced in the fragmentation of 500 MeV/u ^{46}Ti. *Z. Phys.* **1994**, *350*, 215–219. [CrossRef]
19. Eisele, J.A.; Larson, R.E. Gamma rays from the decay of ^{44}Sc, ^{44m}Sc and ^{48}Sc and energy levels in "Ca and ^{48}Ti. *J. Radiochim. Acta* **1970**, *14*, 54–55. [CrossRef]
20. Japan Radioisotope Association. *Ratioisotope Pocket Data Book*, 12th ed.; Japan Radioisotope Association: Tokyo, Japan, 2020.
21. Durán, M.T.; Juget, F.; Nedjadi, Y.; Bailat, C.; Grundler, P.V.; Talip, Z.; van der Meulen, N.P.; Casolaro, P.; Dellepiane, G.; Braccini, S. Half-life measurement of ^{44}Sc and ^{44m}Sc. *Appl. Radiat. Isot.* **2022**, *190*, 110507. [CrossRef] [PubMed]
22. Mikolajczak, R.; Huclier-Markai, S.; Alliot, C.; Haddad, F.; Szikra, D.; Forgacs, V.; Garnuszek, P. Production of scandium radionuclides for theranostic applications: Towards standardization of quality requirements. *EJNMMI Radiopharm. Chem.* **2021**, *6*, 19. [CrossRef] [PubMed]
23. Wibisono; Ningsih, F.R.; Septian, H.; Ragaguci. Evaluation of the fractionation process on aviation turbine fuel production using nuclear technology. *J. Phys. Conf. Ser.* **2020**, *1511*, 012086. [CrossRef]
24. Prohaska, T.; Irrgeher, J.; Benefield, J.; Bohlke, J.K.; Chesson, L.; Coplen, T.B.; Ding, T.; Dunn, P.J.H.; Groning, M.; Holden, N.E.; et al. Standard atomic weights of the elements 2021 (IUPAC Technical Report). *Pure Appl. Chem.* **2022**, *94*, 573–600. [CrossRef]
25. Farooq, F.; Nabi, J.U.; Shehzadi, R. β-decay properties of some astrophysically important Sc-isotopes. *Astrophys. Space Sci.* **2021**, *366*, 86. [CrossRef]
26. Bevelacqua, J. Decay Characteristics of Neutron Excess Scandium Nuclei. *Qeios* **2024**. [CrossRef]
27. Tarasov, O.B.; Ahn, D.S.; Bazin, D.; Fukuda, N.; Gade, A.; Hausmann, M.; Inabe, N.; Ishikawa, S.; Iwasa, N.; Kawata, K.; et al. Discovery of ^{60}Ca and Implications For the Stability of ^{70}Ca. *Phys. Rev. Lett.* **2018**, *121*, 022501. [CrossRef] [PubMed]
28. Zhu, S.; Huang, Z.; Hu, Q.; Xu, L. Pressure tuned incommensurability and guest structure transition in compressed scandium from machine learning atomic simulation. *Phys. Chem. Chem. Phys.* **2022**, *24*, 7007–7013. [CrossRef] [PubMed]
29. Kazakov, A.G.; Ekatova, T.Y.; Babenya, J.S. Photonuclear production of medical radiometals: A review of experimental studies. *J. Radioanal. Nucl. Chem.* **2021**, *328*, 493–505. [CrossRef]
30. Kaneda-Nakashima, K.; Zhang, Z.; Nagata, K.; Shirasaki, K.; Kikunaga, H.; Yamamura, T.; Ooe, K.; Watabe, T.; Toyoshima, A.; Yoshimura, T.; et al. Dispersion of Alpha-Nuclides during animal experiments. *Radiat. Saf. Manag.* **2021**, *20*, 29–38. [CrossRef]
31. Fathi, F.; Moghaddam-Banaem, L.; Shamsaei, M.; Samani, A.; Maragheh, M.G. Production, biodistribution, and dosimetry of ^{47}Sc-1,4,7,10-tetraazacyclododecane- 1,4,7,10-tetramethylene phosphonic acid as a bone-seeking radiopharmaceutical. *J. Med. Phys.* **2015**, *40*, 156–164. [CrossRef] [PubMed]
32. Kim, D.M.; Lee, S.Y.; Lim, J.C.; Cho, E.H.; Park, U.J. RUNX3 regulates the susceptibility against EGFR-targeted non-small cell lung cancer therapy using ^{47}Sc-conjugated cetuximab. *BMC Cancer* **2023**, *23*, 652. [CrossRef] [PubMed]
33. Nardo, L.D.; Pupillo, G.; Mou, L.; Furlanetto, D.; Rosato, A.; Esposito, J.; Meléndez-Alafort, L. Preliminary dosimetric analysis of DOTA-folate radiopharmaceutical radiolabelled with ^{47}Sc produced through ^{nat}V(p,x)^{47}Sc cyclotron irradiation. *Phys. Med. Biol.* **2021**, *66*, 025003. [CrossRef] [PubMed]
34. Vaughn, B.A.; Loveless, C.S.; Cingoranelli, S.J.; Schlyer, D.; Lapi, S.E.; Boros, E. Evaluation of ^{177}Lu and ^{47}Sc Picaga-Linked, Prostate-Specific Membrane Antigen-Targeting Constructs for Their Radiotherapeutic Efficacy and Dosimetry. *Mol. Pharm.* **2021**, *18*, 4511–4519. [CrossRef] [PubMed]
35. Meier, J.P.; Zhang, H.J.; Freifelder, R.; Bhuiyan, M.; Selman, P.; Mendez, M.; Kankanamalage, P.H.A.; Brossard, T.; Pusateri, A.; Tsai, H.M.; et al. Accelerator-Based Production of Scandium Radioisotopes for Applications in Prostate Cancer: Toward Building a Pipeline for Rapid Development of Novel Theranostics. *Molecules* **2023**, *28*, 6041. [CrossRef] [PubMed]
36. Garnuszek, P.; Karczmarczyk, U.; Maurin, M.; Sikora, A.; Zaborniak, J.; Pijarowska-Kruszyna, J.; Jaroń, A.; Wyczółkowska, M.; Wojdowska, W.; Pawlak, D.; et al. PSMA-D4 Radioligand for Targeted Therapy of Prostate Cancer: Synthesis, Characteristics and Preliminary Assessment of Biological Properties. *Int. J. Mol. Sci.* **2021**, *22*, 2731. [CrossRef] [PubMed]
37. Moghaddam-Banaem, L.; Deilami-Nezhad, L.; Sadeghi, M.; Jalilifar, M. Development and estimation of human dosimetry of a new ^{47}Sc-risedronate for radiopharmaceutical application. *Radiat. Prot. Dosim.* **2022**, *198*, 1483–1494. [CrossRef] [PubMed]
38. Cingoranelli, S.J.; Putnam, E.; Houson, H.A.; Gimblet, G.R.; Samuel, S.; Tekin, V.; Lapi, S.E. Investigating the Theranostic Potential of Elementally Matched [^{43}Sc]Sc-PSMA-617 and [^{47}Sc]Sc-PSMA-617. *Mol. Pharm.* **2026**, *23*, 1517–1528. [CrossRef] [PubMed]

39. Andersson, M.; Johansson, L.; Eckerman, K.; Mattsson, S. IDAC-Dose 2.1, an internal dosimetry program for diagnostic nuclear medicine based on the ICRP adult reference voxel phantoms. *EJNMMI Res.* **2017**, *7*, 88. [CrossRef] [PubMed]
40. Koning, A.J.; Rochman, D.; Sublet, J.C.; Dzysiuk, N.; Fleming van der Marck, S. TENDL: Complete Nuclear Data Library for Innovative Nuclear Science and Technology. *Nucl. Data Sheets* **2019**, *155*, 1–55. [CrossRef]
41. Aliev, R.A.; Belyshev, S.S.; Furkina, E.B.; Khankin, V.V.; Kuznetsov, A.A.; Dzhilavyan, L.Z.; Priselkova, A.B.; Ishkhanov, B.S. Photonuclear production of medically relevant radionuclide ^{47}Sc. *Radioanal. Nucl. Chem.* **2020**, *326*, 1099. [CrossRef]
42. Hovhannisyan, G.H.; Bakhshiyan, B.M.; Balabekyan, A.R.; Kerobyan, I.A. Production of ^{47}Sc in photonuclear reactions on ^{nat}Ti targets at the bremsstrahlung endpoint energy of 30 and 40 MeV. *Appl. Radiat. Isot.* **2022**, *182*, 110138. [CrossRef] [PubMed]
43. Zheltonozhsky, V.O.; Savrasov, A.M.; Slisenko, V.I.; Myznikov, D.E. Investigation of (γ, xpxn)-reactions on titanium, lutetium, nickel and chromium nuclei at E_{br}=37 MeV. *Radiat. Phys. Chem.* **2024**, *216*, 111387. [CrossRef]
44. Benabdallah, N.; Zhang, H.; Unnerstall, R.; Fears, A.; Summer, L.; Fassbender, M.; Rodgers, B.E.; Abou, D.; Radchenko, V.; Thorek, D.L.J. Engineering a modular ^{44}Ti/^{44}Sc generator: Eluate evaluation in preclinical models and estimation of human radiation dosimetry. *EJNMMI Res.* **2023**, *13*, 17. [CrossRef] [PubMed]
45. Colclough, N.; Ruston, L.; Wood, J.M.; MacFaul, P.A. Species differences in drug plasma protein binding. *Med. Chem. Comm.* **2014**, *5*, 963. [CrossRef]
46. Alashga, H.; Albenmousa, A.; Peedikayil, M.; Abougamel, M.; Alfadda, A.; Alsohaibani, F.; Alkahtani, K.; AlAjlan, B.; Abaalkhail, F.; Al-Saleh, I. The biliary and urinary excretion pattern of toxic and essential metals in patients with biliary and liver diseases and its association with fibrosis-4 index. *Met. Res.* **2023**, *3*, note01–note18. [CrossRef]
47. Ford-Hutchinson, A.W.; Perkins, D.J. The Binding of Scandium Ions to Transferrin in vivo and in vitro. *Eur. J. Biochem.* **1971**, *21*, 55–59. [CrossRef] [PubMed]
48. Li, H.; Sadler, P.J.; Sun, H. Rationalization of the strength of metal binding to human serum transferrin. *Eur. J. Biochem.* **1996**, *242*, 387–393. [CrossRef] [PubMed]
49. Hirata, S.; Echigo, H.; Munekane, M.; Mishiro, K.; Washiyama, K.; Fuchigami, T.; Wakabayashi, H.; Takahashi, K.; Kinuya, S.; Ogawa, K. Engineering a Radiohybrid PSMA Ligand with an Albumin-Binding Moiety and Pharmacokinetic Modulation via an Albumin-Binding Competitor for Radiotheranostics. *Molecules* **2025**, *30*, 2804. [CrossRef] [PubMed]
50. Watanabe, A.; Fujino, S.; Takaki, N. Feasibility of Mass Production of Lu-177 Using Commercial Light Water Reactors. *J. Nucl. Sci. Technol.* **2026**, *25*, 65–73. (In Japanese) [CrossRef]
51. Nagai, Y.; Kawabata, M.; Hashimoto, S.; Tsukada, K.; Hashimoto, K.; Motoishi, S.; Saeki, H.; Motomura, A.; Minato, F.; Itoh, M. Estimated Isotopic Compositions of Yb in Enriched ^{176}Yb for Producing ^{177}Lu with High Radionuclide Purity by ^{176}Yb(d,x)^{177}Lu. *J. Phys. Soc. Jpn.* **2022**, *91*, 044201. [CrossRef]
52. *IAEA-TECDOC-934*; Effects of Ionizing Radiation on Blood and Blood Components: A Survey. IAEA: Vienna, Austria, 1997.

Disclaimer/Publisher's Note: The statements, opinions and data contained in all publications are solely those of the individual author(s) and contributor(s) and not of MDPI and/or the editor(s). MDPI and/or the editor(s) disclaim responsibility for any injury to people or property resulting from any ideas, methods, instructions or products referred to in the content.